Macromolecular Research (2023) 31:625–633
https://doi.org/10.1007/s13233-023-00158-1

Online ISSN 2092-7673
Print ISSN 1598-5032

ARTICLE

Fast-response thermo-sensitive actuator based on asymmetric structured PNIPAM hydrogel with inorganic particles embedding

Zhuanzhuan Fan[1] · Weizhong Xu[1] · Ruofei Wang[1] · Huaping Wu[2] · Aiping Liu[1]

Received: 25 September 2022 / Revised: 21 November 2022 / Accepted: 11 December 2022 / Published online: 3 April 2023

Abstract

Hydrogel actuators have potential applications in many fields because of their multiple responsiveness to environmental stimuli. However, it is still very challenging to design a hydrogel actuator with simple preparation, fast response, and good mechanical properties. In this work, a facile and convenient method to obtain a fast responsive hydrogel actuator has been successfully developed by embedding uniform inorganic particles into Poly(N-isopropylacrylamide) hydrogel network to form an asymmetric structure. By controlling the types and contents of inorganic particles, a wide range of adjustable actuation property can be achieved. At the same time, the introduction of inorganic particles greatly increases the mechanical properties of hydrogels, which is also very important for actuation performance improvement of hydrogel actuators. The optimized hydrogel exhibits relatively fast bending deformation under thermal stimulation (60 ℃), with a bending velocity of about 13.0° s^{-1} within first 10 s and a bending amplitude of about 328.1° within 1 min. The hydrogel can be designed to be temperature-controlled claw actuators with programmable shapes, indicating its application prospects in encapsulating, grasping, and transporting objects in water environment.

Graphical Abstract

We successfully designed and manufactured hybrid hydrogels with an asymmetric structure and improved mechanical property by adding inorganic particles to the PNIPAM hydrogel. The hybrid hydrogel with optimized SiO_2 particles shows superior actuation properties due to bigger different in the swelling rates on both sides of hybrid hydrogels. The flexible and controllable deformation of the hydrogel actuator provides an inspiration for intelligent soft actuator in water environmental applications.

✉ Aiping Liu
liuaiping1979@gmail.com

[1] Key Laboratory of Optical Field Manipulation of Zhejiang Province, Zhejiang Sci-Tech University, Hangzhou 310018, People's Republic of China

[2] Key Laboratory of Special Purpose Equipment and Advanced Processing Technology, Ministry of Education and Zhejiang Province, College of Mechanical Engineering, Zhejiang University of Technology, Hangzhou 310023, People's Republic of China

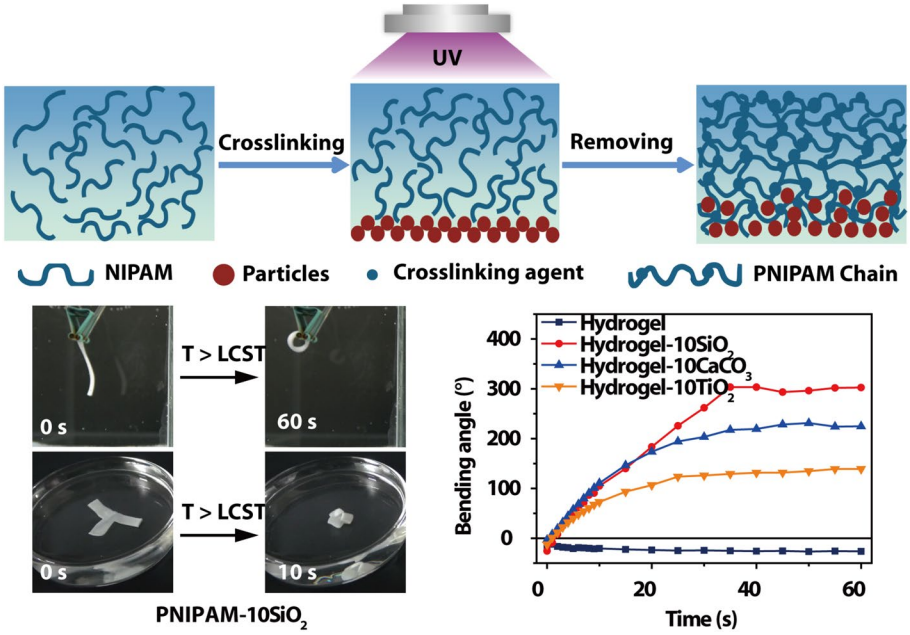

Keywords Asymmetric structure · Hydrogel actuator · Thermo-sensitive behavior · Inorganic particles

1 Introduction

Inspired by the deformation principles of natural organisms [1], such as crawling, swimming, and flying, soft actuators have been widely developed and shown broad application prospects in the fields of drug release [2], valve [3], soft robot [4–7], and so on [8]. Currently, the hydrogel is regarded as one of the excellent candidates as soft actuators because of its captivating characteristics, such as perfect matching with the flexible organisms, good withstanding to large strains, strong impact resistance, excellent environmental adaptability, and strong safety in human–computer interaction. The main reason for bending/straightening of hydrogels under external stimulus is the non-equilibrium stress generated by the inhomogeneous strain in the hydrogels when subjected to environmental stimuli (such as temperature [9–12], light [13, 14], pH [15, 16], electricity [17–19], magnetic field [20], and so on [21]). The deformation of isotropy hydrogels is mainly confined to simple volume expansion/contraction, which greatly limits their application scope. Therefore, the strategy of preparing hydrogel actuators with anisotropic structure is highly desired.

In order to obtain anisotropic hydrogel actuators, one of the effective strategies is to directly assemble two or more layers of hydrogels with different structures or properties [11–13, 22, 23]. Chen et al. designed two-layer hydrogel actuators with different responses to temperature by imitating the closure of natural mimosa plants [12]. However, the poor adhesion at the interface between layers often results in delamination, which limits the recycling of hydrogels and recoverable deformation. Another useful method is to design a monolayer hydrogel actuator with an inhomogeneous internal structure [24–32]. For example, Chen et al. prepared a responsive hydrogel with a well-defined gradient pore structure using a hydrothermal process, where the encapsulated polypyrrole nanoparticles as photothermal transducers made the hydrogel actuator directional laser-response and programmable locomotion [14]. The porous gradient structure of hydrogel could also effectively adjust the bending speed and deformation degree of hydrogel actuators to realize designed actuation. Michael et al. obtained a gradient distribution of hydrogels by introducing polystyrene (PS) microspheres into the Poly(N-isopropylacrylamide) (PNIPAM) hydrogel precursor solution via an external electric field, presenting controllable bending of hydrogel toward the side with low-concentration PS under the temperature of lower critical solution temperature (LCST) [26]. Liu et al. introduced titanate nanosheets (TINSS) into the PNIPAM hydrogel under the help of an external magnetic field (10 T), obtaining the TINSS-PNIPAM-based peristaltic soft robot [30]. In addition, researchers have developed other construction methods, such as 3D printing [33, 34], self-assembly [35–37], and surface pattering [38–40], to enrich the preparation methods of hydrogel actuators. However, the

major weakness of the existing preparation methods for heterogeneous hydrogels lies in their complex operation, high cost, and difficult to control performance, which may limit the practical application of hydrogel actuators. Therefore, it is crucial and challenging to prepare hydrogel actuators with both excellent actuating property and great mechanical property by a simple and rapid preparation method.

In this paper, we propose a fascinating method to construct the hybrid hydrogel actuator with an asymmetric structure by embedding inorganic particles (SiO_2, TiO_2, and $CaCO_3$) into PNIPAM hydrogel network. The hydrogel not only responds quickly to temperature change but also has excellent mechanical property. Compared with the pure PNIPAM hydrogel, the hybrid hydrogel generates a bigger driving force and shows significant bending/straightening behaviors with adjustable shapes of claw actuators, which can be applied to grasp, encapsulate, and transport target objects. This provides an applicable strategy for the design and manufacture of hydrogel-based actuators.

2 Experimental

2.1 Materials

NIPAM monomer, methanol (CH_3OH), silica (SiO_2), titanium dioxide (TiO_2), and calcium carbonate ($CaCO_3$) were all purchased from Shanghai Macklin Biochemical Co. Ltd (China). The synthetic hectorite "Laponite XLG" ($[Mg_{5.34}Li_{0.66}\ Si_8O_{20}(OH)_4]Na_{0.66}$) and 1-Hydroxycyclohexyl phenyl ketone (Irg. 184) were obtained from Nanocor Inc. (USA) and Shanghai Aladdin Chemical Agent Co., Ltd (China), respectively.

2.2 Preparation of pure PNIPAM hydrogel

Firstly, a homogeneous hydrogel precursor solution containing monomers NIPAM (5.65 g), cross-linker (Laponite XLG, 1.14 g), and photoinitiator Irg.184 (0.226 g) was prepared. Subsequently, the precursor solution was injected into the funnel of the glass vacuum filter and chemically cross-linked under the top-down UV irradiation (365 nm, 250 W) for 4 min to obtain the pure PNIPAM hydrogel. Finally, the as-prepared sample was immersed in deionized water until reaching swelling equilibrium.

2.3 Preparation of PNIPAM-nSiO_2 hydrogels

A certain amount of SiO_2 solution (10 nm in diameter, 5 mg mL^{-1}) was prepared and continuously filtered by a Glassware Vacuum Filter for 5 min to obtain a filter membrane with uniformly dispersed SiO_2 particles. Subsequently, 2.5 mL NIPAM precursor solution was uniformly dropped on the surface of the filter membrane containing SiO_2 particles. After UV cross-linking (365 nm, 250 W) the mixture for 4 min, the hydrogel was slowly removed from the filtration membrane, and the surface of the hydrogel was cleaned with deionized water. Finally, the hydrogels with the asymmetric structure were obtained (Fig. 1a). In order to research the effect of SiO_2 particle contents on the microstructure and properties of hydrogels, the volume of SiO_2 solution for vacuum filtration was controlled to be 1, 3, 5, 10, 15, 20, and 30 mL, respectively. Therefore, the obtained hydrogels were encoded as PNIPAM-nSiO_2 ($n = 1, 3, 5, 10, 15, 20, 30$).

2.4 Preparation of PNIPAM-mTiO_2 and PNIPAM-m$CaCO_3$ hydrogels

In order to explore the effect of different kinds of inorganic particles on the microstructure and macroscopic properties of the hydrogels, we prepared PNIPAM-mTiO_2 and PNIPAM-m$CaCO_3$ hydrogels by adding TiO_2 particle (20 nm in diameter) and $CaCO_3$ particle (20 nm in diameter) solutions (5 mg mL^{-1}, m was the volume of solution), respectively.

2.5 Preparation of PNIPAM-10SiO_2 hydrogel-based grippers

In order to explore the application of hydrogel actuator, the PNIPAM-10SiO_2 hydrogels were cut into three-claw, four-claw, five-claw, and pentagram shapes as grippers.

2.6 Characterization

The surface morphologies of hydrogels were observed using a scanning electron microscope (SEM, S-4800, Hitachi, Japan) at an accelerated voltage of 5 kV after the hydrogels were frozen in liquid nitrogen and then freeze-dried with a freeze drier (FD-1A-80, Shanghai Leewen Scientific Instrument Co., Ltd., China) at − 90 °C for about 24 h. The surface roughness (*R*a value) was measured by using a laser scanning microscope (VK-X100, Keyence Inc., Japan). The mechanical properties of hydrogel were investigated by tensile tests using Microcomputer Control Electronic Universal Material Testing Machine (MX-0350, Jiangsu Moxin Industrial System Co., Ltd., China). The LCST of the hybrid hydrogels was analyzed on a differential scanning calorimeter (DSC, TA DSC Q200, USA) by heating the sample from 10 ℃ to 40 ℃ with the heating rate of 10 ℃/min under nitrogen.

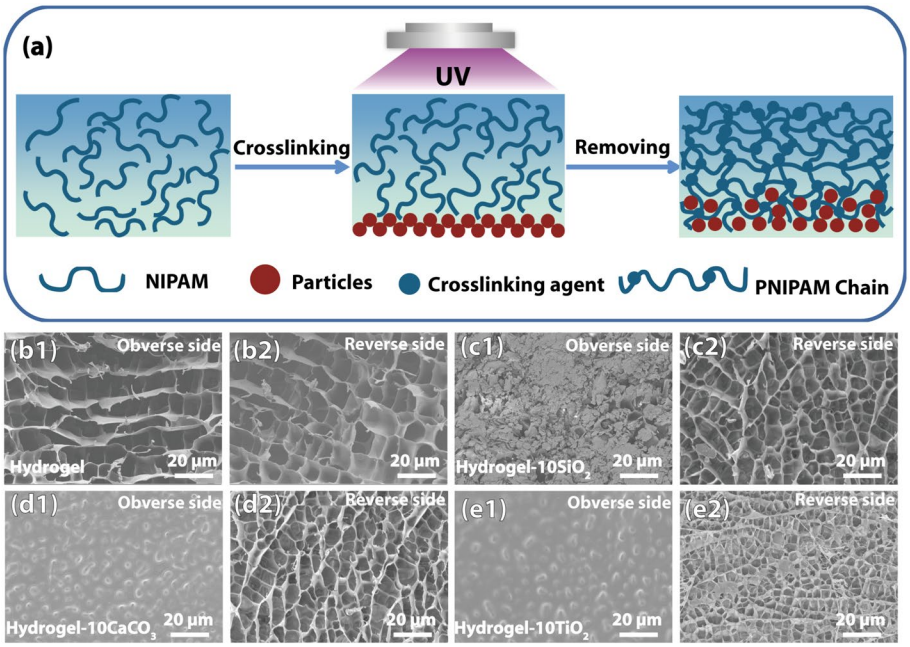

Fig. 1 **a** Schematic preparation process of the hybrid hydrogels. SEM images of (b1) obverse and (b2) reverse sides of pure PNIPAM hydrogel; SEM images of (c1) obverse and (c2) reverse sides of PNIPAM-10SiO_2 hydrogel; SEM images of (d1) obverse and (d2) reverse sides of PNIPAM-10$CaCO_3$ hydrogel; SEM images of (e1) obverse and (e2) reverse sides of PNIPAM-10TiO_2 hydrogel. The side that contacts the particles is defined as the obverse side of the hydrogel and the other side as the reverse side

To explore the actuation behaviors of the hydrogel, the tested hydrogel was cut into rectangular strips with the size 30 mm × 10 mm × 1 mm (length × width × thickness). One end of the long axis of the hydrogel was held in place with a small clip, while the other end of the hydrogel was suspended freely. The bending of hydrogels in deionized water at 60 ℃ and their recovery at room temperature were observed and recorded by a digital camera (FDR-AX45, SONY, Japan). The open source software Image J was used to analyze the bending angle (θ) of hydrogel at different times (t), and the relationship between bending angle and time was obtained. The bending angle was related to the central angle of the circular arc in the deformation zone. The bending amplitude was calculated by measuring the angle difference between the maximum bending angle and the initial bending angle [41]. The ratio of bending angle to corresponding time period was defined as the bending velocity. To ensure the reliability of the results, the above tests were repeated several times.

3 Results and discussion

3.1 Morphology of thermo-sensitive hybrid hydrogels

Since inorganic particles have large specific surface area and strong interfacial interaction with polymers, the introduction of inorganic particles in polymers can provide alternative ideas for the design and preparation of hydrogel actuators with anisotropic structures [42]. Fig. 1b-e shows morphologies of the hybrid hydrogels with different inorganic particles embedded into PNIPAM hydrogels to construct asymmetric structure (the volume of particle solution for vacuum filtration is all controlled to be 10 mL). According to the SEM images of pure PNIPAM hydrogel without inorganic particles, it can be seen that the hydrogel exhibits a uniform pore structure with an aperture of about 10 μm on the obverse side and reverse side (Fig. 1b1, 2). Compared with the isotropic network structure of pure PNIPAM hydrogel, the hydrogel with inorganic particles on the obverse shows an asymmetric porous structure, namely, the obverse side is almost filled with the granular particles, while the reverse side still remains the porous structure just like the pure hydrogel (Fig. 1c–e). The asymmetric structures of the hybrid hydrogels are further proved by element distribution (Si, Ca, and Ti) along the thickness direction of hydrogels (Figure S1), which provides a prerequisite for the bending deformation of the hydrogel under external stimulation.

To further verify the asymmetric structure of the hybrid hydrogels, we observed the surfaces of the hydrogels by the laser scanning microscope. As shown in Fig. 2a, both the obverse and reverse sides of pure PNIPAM hydrogel are relatively smooth without obvious difference. The images of hydrogels containing different inorganic particles (Fig. 2b–d) show that the difference in the roughness of both sides of PNIPAM-10SiO_2 hydrogel is largest, followed by PNIPAM-10$CaCO_3$ hydrogel, and PNIPAM-10TiO_2 hydrogel has the smallest roughness difference. This is because that the relative smaller and more SiO_2 particles can easily pack into the porous structures and better integrate with the hydrogel network, resulting in agglomerated clusters on the obverse surface of PNIPAM-10SiO_2 hydrogel.

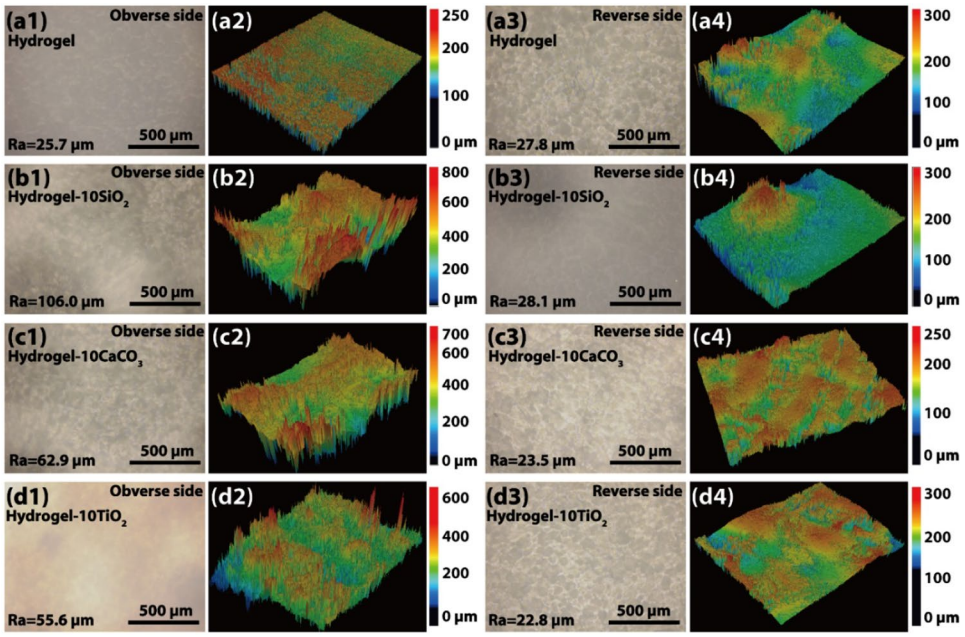

Fig. 2 Laser scanning microscope images of (a1–d1) obverse sides and (a3–d3) reverse sides of **a** pure PNIPAM hydrogel, **b** PNIPAM-10SiO_2 hydrogel, **c** PNIPAM-10$CaCO_3$ hydrogel, and **d** PNIPAM-10TiO_2 hydrogel. Three-dimensional surface profiles of (a2–d2) obverse sides and (a4–d4) reverse sides of corresponding hydrogels

3.2 Mechanical property of thermos-sensitive hydrogels

Stable mechanical properties are of importance for hydrogel-based actuators. Considering the difference of particle types, tensile tests were carried out on pure PNIPAM, PNIPAM-10SiO_2, PNIPAM-10$CaCO_3$, and PNIPAM-10TiO_2 hydrogels. The stress–strain curves of these hydrogels are shown in Fig. 3a. Compared with pure hydrogel, the stress of the hybrid hydrogels with inorganic particles embedding is increased by about two or three times. This is because that the smaller the particle size of inorganic particles, the larger the specific surface area, and the stronger the interaction between inorganic particles and polymer interface, which improves the tensile strength of hybrid hydrogels. However, the embedding of inorganic particles leads to uneven stress distribution on the surface of hydrogels, so that the strain of hybrid hydrogels decreases slightly compared with pure hydrogels (Fig. 3b). In addition, we find that the hybrid hydrogels have higher Young's modulus (Fig. 3c). The improved mechanical properties of hybrid hydrogels would favor better actuation behavior of the hydrogels in the bending deformation process.

3.3 Actuation behavior of thermo-sensitive hydrogels

The actuation property of hydrogels is greatly affected by the asymmetric structure. As a typical thermal responsive polymer, PNIPAM hydrogel contains a certain proportion of hydrophilic amide groups and hydrophobic isopropyl groups in its side chain. The change of temperature will affect the interaction between these groups and water, so that the hydrogel will produce volumetric phase transformation at a lower critical solution temperature (LCST). When the external temperature exceeds LCST, the hydrogel shrinks and forms a hydrophobic state due to the destruction of the hydrophilic/hydrophobic balance in the network structure.

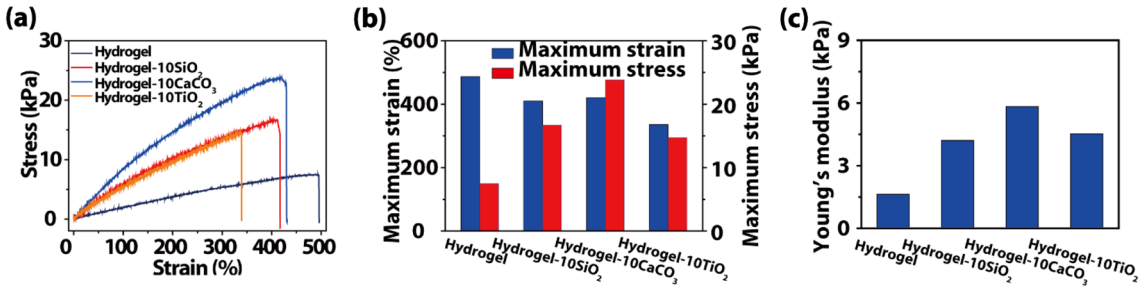

Fig. 3 **a** Tensile stress–strain curves, **b** maximum strain and maximum stress, and **c** Young's modulus of pure PNIPAM, PNIPAM-10SiO_2, PNIPAM-10$CaCO_3$, and PNIPAM-10TiO_2 hydrogels

Conversely, when the external temperature is lower than LCST, the hydrogel absorbs water and expands, showing hydrophilicity [41, 43, 44]. When different kinds of inorganic particles are embedded on the surfaces of hydrogels, LCST of hybrid hydrogels decreases to different degrees when compared with pure hydrogel, and the hydrogels containing inorganic particles show a lower heat flow, especially for the PNIPAM-10SiO_2 which shows a more obvious difference between the top side and the bottom side (Figure S2). This can be attributed to the structure difference on both sides of hybrid hydrogels. The inorganic particles in the hydrogel will block the flow channel of free water after being stimulated by temperature, resulting in different thermal-response volume change rates on both sides of hybrid hydrogels and finally actuating deformation. Therefore, we study the actuation process of hybrid hydrogels in hot water at 60℃ and cold water at about 20℃ in this work by measuring the bending angle-time relations, bending amplitude and bending velocity of hydrogel actuators.

3.3.1 Effect of particle types on actuation property

The actuation properties of hybrid hydrogels are affected by the types of inorganic particles. Pure PNIPAM hydrogel only shows dehydration-induced shrinkage without bending deformation in hot water at 60 ℃ (Fig. 4a). When inorganic particles are embedded as fillers on one side of the hydrogel surface and result in an asymmetric structure, inorganic particles constitute a water loss barrier, leading to the bending and deformation of hydrogel toward the side of the hydrogel without inorganic particles (reverse side to the left and obverse side to the right) in hot water, and then gradually return to the initial state in room temperature water (Fig. 4b–d). Compared with the PNIPAM-10TiO_2 and PNIPAM-10$CaCO_3$ composite hydrogel, PNIPAM-10SiO_2 hydrogel exhibits excellent bending deformation with bending velocity of about 13.0°s^{-1} within first 10 s and bending amplitude of about 328.1° within 1 min when it is placed in hot water (60 ℃) under the equilibrium state of swelling (Fig. 4e, f). The recovery velocity is also faster within first 2 min in cold water (Fig. 4g, h). This may be because of more compact structure and rougher surface in the obverse side of PNIPAM-10SiO_2 hydrogel, which might block more flow channel of free water under temperature stimulation, resulting in bigger different in the swelling rates on both sides of the hybrid hydrogel.

3.3.2 Effect of SiO_2 particle contents on actuation property

The contents of SiO_2 particles also have a great influence on the actuation properties of PNIPAM-nSiO_2 hydrogels. With the content increase of SiO_2 particles, the actuation properties of the PNIPAM-nSiO_2 hydrogels increase first and then decrease in the bending amplitude and bending speed with

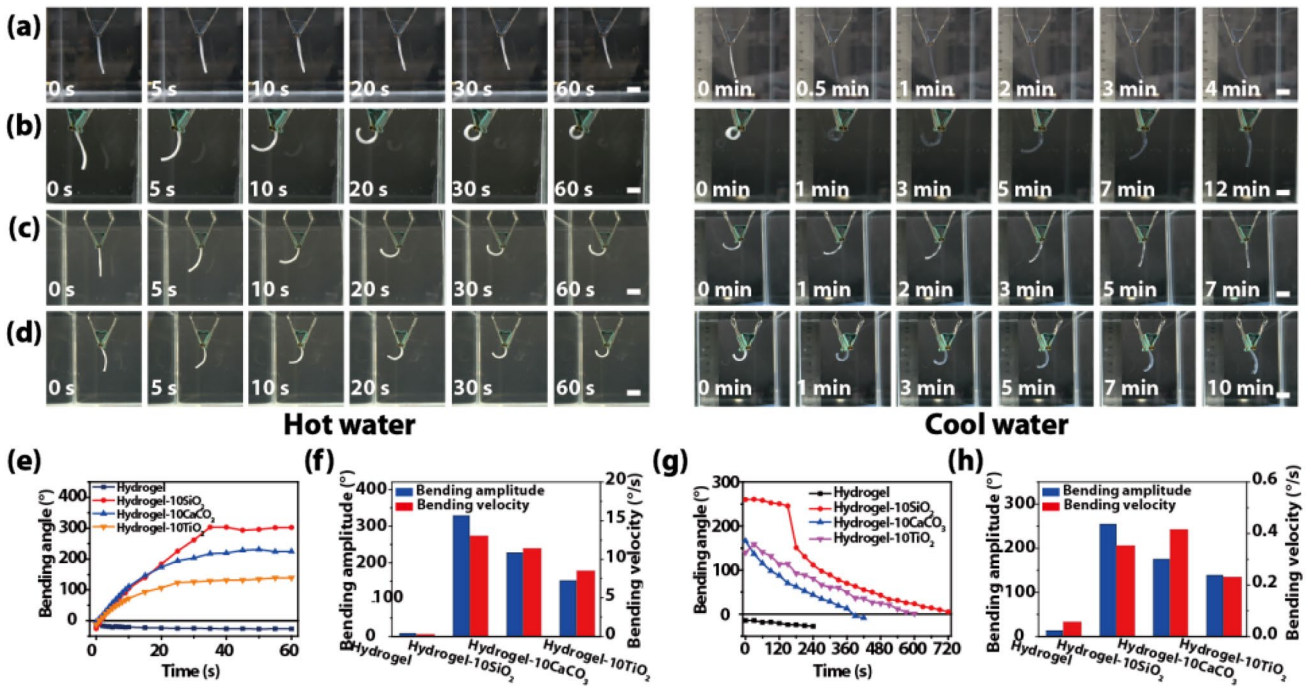

Fig. 4 The bending behaviors of **a** pure PNIPAM, **b** PNIPAM-10SiO_2, **c** PNIPAM-10$CaCO_3$, and **d** PNIPAM-10TiO_2 hydrogels. The scale bar is 1 cm. The relationship between the bending angle and time of different actuators in **e** hot water or **g** cool water, respectively. The bending amplitude and the bending velocity of different actuators in **f** hot water or **h** cool water, respectively

the optimal value obtained for PNIPAM-10 SiO_2 hydrogel (Figs. 4f and 5a–i). As the content of SiO_2 particles gradually increases, the water loss resistance of the rough surface of the hydrogel gradually increases, resulting in a greater actuating force. However, when the content of SiO_2 particles exceeds a certain limit, the greater gravity of SiO_2 particles in the hydrogel will hinder the further bending of hydrogel. Compared with other hydrogel actuators reported previously, the PNIPAM-10SiO_2 hydrogel prepared by us has fast response speed and large bending amplitude, indicating that the actuation properties of the hybrid hydrogel can be effectively adjusted by using appropriate inorganic particle types and contents for better use as actuator (Fig. 5j).

3.4 Applications of thermo-sensitive hybrid hydrogel

In order to verify the feasibility of the hybrid hydrogels applied in practical working environment, hydrogel actuators, namely, temperature-controlled gripper actuators, were well designed. The PNIPAM-10SiO_2 hydrogel samples (round shape) were cut into claws and placed in water environment, and the bending processes in hot water were recorded by camera. As shown in Fig. 6a–d, the hydrogel actuators with three-claw, four-claw, five-claw, and pentagram shapes completely close like a claw after about 10 s in 60 ℃ water. The gripper actuators generally respond quickly and can mimic the grasping action of human hand well, indicating their application potential as soft grippers in the treatment of easily fragile or scratched objects [45].

4 Conclusions

In summary, we report a simple and rapid preparation method to obtain thermo-sensitive actuators of hybrid hydrogels with asymmetric structure by embedding inorganic particles into PNIPAM hydrogels. The hybrid PNIPAM hydrogels present granular and microporous structures at two surfaces, respectively, causing bending deformation of hydrogel toward microporous side under temperature stimulation. The actuation properties of hydrogels can be widely adjusted by changing the content and type of inorganic particles. Due to the blockage of more free water channels, the swelling rate difference between the two sides of the optimized PNIPAM-10SiO_2 hybrid hydrogels are greater, showing better actuation properties with the bending velocity about 13.0°s^{-1} within 10 s and the bending amplitude about 328.1° within 1 min. In addition, the flexible and controllable deformation of the hydrogel actuator is realized by designing hydrogel grippers with different shapes. This method has the advantages of simple preparation, low cost, and programmable operation, which provides an inspiration for intelligent soft actuator design in water environmental applications.

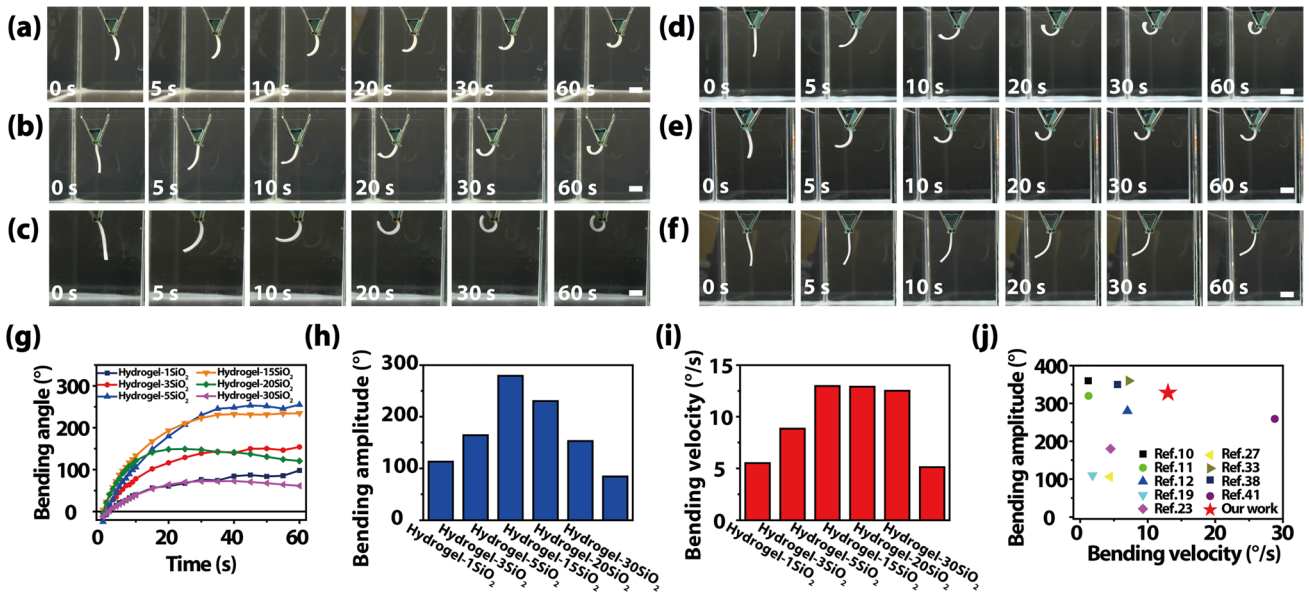

Fig. 5 The bending behaviors of **a** PNIPAM-1SiO_2, **b** PNIPAM-3SiO_2, **c** PNIPAM-5SiO_2, **d** PNIPAM-15SiO_2, **e** PNIPAM-20SiO_2, and **f** PNIPAM-30SiO_2 hydrogels. **g** The relationship between the bending angle and time of different actuators in hot water. **h** The bending amplitude and **i** the bending velocity of different actuators in hot water. **j** Comparison of bending amplitude and bending velocity between our prepared hydrogel actuator and other previously reported hydrogel actuators

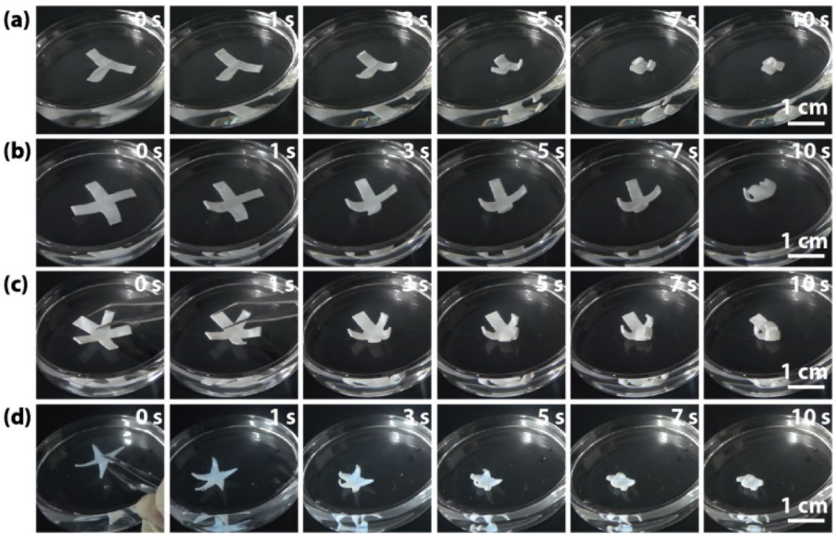

Fig. 6 Application of thermo-sensitive PNIPAM-10SiO_2 hydrogel as soft actuators with **a** three-claw, **b** four-claw, **c** five-claw, and **d** pentagram shapes

Supplementary Information The online version contains supplementary material available at https://doi.org/10.1007/s13233-023-00158-1.

Acknowledgements This work was supported by the National Natural Science Foundation of China (Nos. 12272351, 11672269 and 11972323), the Zhejiang Outstanding Youth Fund of China (No. LR19E020004), the Youth Top-notch Talent Project of Zhejiang Ten Thousand Plan of China (No. ZJWR0308010), and the Zhejiang Provincial Natural Science Foundation of China (No. LR20A020002).

Declarations

Conflict of interest The authors state that they have no conflict of interest.

References

1. X.X. Le, W. Lu, J.W. Zhang, T. Chen, Adv. Sci. **6**, 1801584 (2019)
2. H. Li, G. Go, S.Y. Ko, J.-O. Park, S. Park, Smart Mater. Struct. **25**, 027001 (2016)
3. Q. Yu, J.M. Bauer, J.S. Moore, D.J. Beebe, Appl. Phys. Lett. **78**, 2589 (2001)
4. H. Yuk, S.T. Lin, C. Ma, M. Takaffoli, N.X. Fang, X.H. Zhao, Nat. Commun. **8**, 14230 (2017)
5. W. Francis, A. Dunne, C. Delaney, L. Florea, D. Diamond, Sens. Actuators B Chem. **250**, 608 (2017)
6. C.N. Kedir, D. Salinas-Torres, A.F. Quintero-Jaime, A. Benyoucef, E. Morallon, J. Mol. Struct. **1248**, 131445 (2022)
7. L. Hua, M. Xie, Y. Jian, B. Wu, C. Chen, C. Zhao, A.C.S. Appl, Mater. Interfaces **11**, 43641 (2019)
8. X. Song, G. Lu, J. Wang, J. Zheng, S. Sui, Q. Li, Y. Zhang, Molecules **27**, 5326 (2022)
9. P. Dong, W. Xu, Z. Kuang, Y. Yao, Z. Zhang, D. Guo, H. Wu, T. Zhao, A. Liu, Adv. Intel. Syst. **3**, 2100030 (2021)
10. J. Liu, L. Jiang, A. Liu, S. He, W. Shao, Sens. Actuators B Chem. **357**, 131434 (2022)
11. J. Zheng, P. Xiao, X.X. Le, W. Lu, P. Théato, C. Ma, B.Y. Du, J.W. Zhang, Y.J. Huang, T. Chen, J. Mater. Chem. C **6**, 1320 (2018)
12. W.J. Zheng, N. An, J.H. Yang, J. Zhou, Y.M. Chen, A.C.S. Appl, Mater. Interfaces **7**, 1758 (2015)
13. M. Kim, J. Choi, S.Y. Kim, Mater. Today Chem. **26**, 101014 (2022)
14. R.C. Luo, J. Wu, N.-D. Dinh, C.-H. Chen, Adv. Funct. Mater. **25**, 7272 (2015)
15. Y.C. Zhang, J.X. Liao, T. Wang, W.X. Sun, Z. Tong, Adv. Funct. Mater. **28**, 1707245 (2018)
16. C.X. Ma, W. Lu, X.X. Yang, J. He, X.X. Le, L. Wang, J.W. Zhang, M.J. Serpe, Y.J. Huang, T. Chen, Adv. Funct. Mater. **28**, 1704568 (2018)
17. Y. Osada, H. Okuzaki, H. Hori, Nature **355**, 242 (1992)
18. D. Morales, E. Palleau, M.D. Dickey, O.D. Velev, Soft Matter **10**, 1337 (2014)
19. H.Y. Jiang, L.X. Fan, S. Yan, F.B. Li, H.J. Li, J.G. Tang, Nanoscale **11**, 2231 (2019)
20. H. Haider, C.H. Yang, W.J. Zheng, J.H. Yang, M.X. Wang, S. Yang, M. Zrinyi, Y. Osada, Z.G. Suo, Q.Q. Zhang, J.X. Zhou, Y.M. Chen, Soft Matter **11**, 8253 (2015)
21. S. Maeda, Y. Hara, T. Sakai, R. Yoshida, S. Hashimoto, Adv. Mater. **19**, 3480 (2007)
22. W. Xu, P. Dong, S. Lin, Z. Kuang, Z. Zhang, S. Wang, F. Ye, L. Cheng, H. Wu, A. Liu, Sens. Actuators B Chem. **359**, 131547 (2022)
23. Q. Zhao, Y.H. Liang, L. Ren, Z.L. Yu, Z.H. Zhang, F. Qiu, L.Q. Ren, J. Mater. Chem. B **6**, 1260 (2018)
24. Z. Chen, Y. Chen, C. Chen, X. Zheng, H. Li, H. Liu, Chem. Eng. J. **424**, 130562 (2021)
25. T.-A. Asoh, M. Matsusaki, T. Kaneko, M. Akashi, Adv. Mater. **20**, 2080 (2008)
26. D. Morales, B. Bharti, M.D. Dickey, O.D. Velev, Small **12**, 2283 (2016)
27. Y. Tan, D. Wang, H.-X. Xu, Y. Yang, X.-L. Wang, F. Tian, P.P. Xu, W.L. An, X. Zhao, S.M. Xu, A.C.S. Appl, Mater. Interfaces **10**, 40125 (2018)
28. T. Inadomi, S. Ikeda, Y. Okumura, H. Kikuchi, N. Miyamoto, Macromol. Rapid Commun. **35**, 1741 (2014)
29. L. Maggini, M.J. Liu, Y. Ishida, D. Bonifazi, Adv. Mater. **25**, 2462 (2013)
30. Y.S. Kim, M.J. Liu, Y. Ishida, Y. Ebina, M. Osada, T. Sasaki, T. Hikima, M. Takata, T. Aida, Nat. Mater. **14**, 1002 (2015)
31. M.J. Liu, Y. Ishida, Y. Ebina, T. Sasaki, T. Hikima, M. Takata, T. Aida, Nature **517**, 68 (2015)
32. L.L. Wu, M. Ohtani, M. Takata, A. Saeki, S. Seki, Y. Ishida, T. Aida, J. Mater. Chem. B **8**, 4640 (2014)

33. S.Y. Zheng, Y.Y. Shen, F.B. Zhu, J. Yin, J. Qian, J.Z. Fu, Z.L. Wu, Q. Zheng, Adv. Funct. Mater. **28**, 1803366 (2018)
34. L.M. Huang, R.Q. Jiang, J.J. Wu, J.Z. Song, H. Bai, B.G. Li, Q. Zhao, T. Xie, Adv. Mater. **29**, 1605390 (2017)
35. H.H. He, S. Averick, P. Mandal, H.J. Ding, S.P. Li, J. Gelb, N. Kotwal, A. Merkle, S. Litster, K. Matyjaszewski, Adv. Sci. **2**, 1500069 (2015)
36. S.M. Zhang, M.A. Greenfield, A. Mata, L.C. Palmer, R. Bitton, J.R. Mantei, C. Aparicio, M.O. de la Cruz, S.I. Stupp, Nat. Mater. **9**, 594 (2010)
37. Y. Kang, J.J. Walish, T. Gorishnyy, E.L. Thomas, Nat. Mater. **6**, 957 (2007)
38. X. Peng, T.Q. Liu, Q. Zhang, C. Shang, Q.-W. Bai, H.L. Wang, Adv. Funct. Mater. **27**, 1701962 (2017)
39. J.J. Bowen, M.A. Rose, A. Konda, S.A. Morin, Angew. Chem. **57**, 1236 (2018)
40. Z.J. Wang, C.N. Zhu, W. Hong, Z.L. Wu, Q. Zheng, Sci. Adv. **3**, 1700348 (2017)
41. J. Liu, W.Z. Xu, Z.W. Kuang, P.L. Dong, Y.X. Yao, H.P. Wu, A.P. Liu, F.M. Ye, J. Mater. Chem. C **8**, 12092 (2020)
42. X.X. Tan, F. Nan, I.O.P. Conf, Ser. Mater. Sci. Eng. **840**, 012002 (2020)
43. L. Tang, L. Wang, X. Yang, Y.Y. Feng, Y. Li, W. Feng, Prog. Mater Sci. **115**, 100702 (2021)
44. X.Y. Liu, J. Liu, S.T. Lin, X.H. Zhao, Mater. Today **36**, 102 (2020)
45. Y. Dong, J. Wang, X.K. Guo, S.S. Yang, M.O. Ozen, P. Chen, X. Liu, W. Du, F. Xiao, U. Demirci, B.F. Liu, Nat. Commun. **10**, 4087 (2019)